

Influence of stiffeners on the buckling behaviour of composite panels subjected to non-uniform edge loads

Sasha Azimi^a , T Rajanna^{a*} , K Asha^a , P.K Ravindra^b , Akshay Prakash Kalgutkar^c 

^aDepartment of Civil Engineering, BMS College of Engineering, Bengaluru 560 019, India. Email: sashaasimi@bmsce.ac.in, t.rajanna@gmail.com, asha.civ@bmsce.ac.in

^bDepartment of Civil Engineering, Government Engineering College, Ramanagar-562159, India. Email: ravindrakravindra@ymail.com

^cDepartment of Civil Engineering, Indian Institute of Technology, Mumbai 400 076, India. Email: akshay_kalgutkar@iitb.ac.in

*Corresponding author

<https://doi.org/10.1590/1679-78258093>

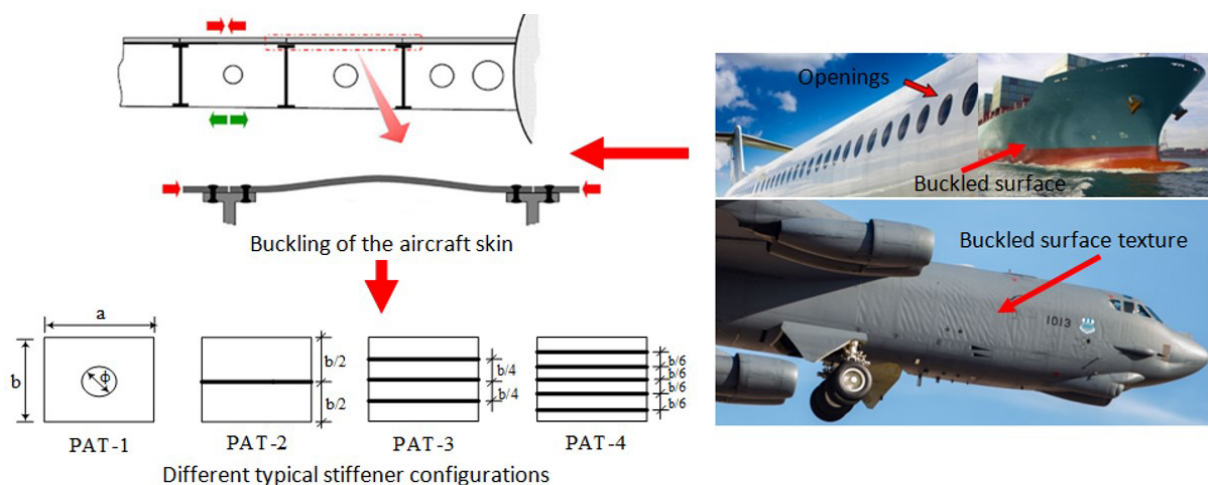
Abstract

Analytical methods for calculating the buckling loads in laminated panels often assume uniform edge loads without any openings, overlooking real-world conditions with diverse non-uniform edge loads and varying cutout sizes. This study aims to explore the buckling behavior of composite panels with and without stiffeners under different non-uniform edge load distributions by developing a robust and computationally efficient finite element (FE) formulation. Buckling loads are determined for different plate aspect ratios, number of stiffeners under various non-uniform edge-loading cases. Furthermore, it addresses the effects of different layup schemes and stiffener eccentricities. The analysis employs a 9-noded heterosis plate element and a compatible 3-noded beam element, incorporating shear deformation and rotary inertia for both the plate and stiffeners. Additionally, due to the non-uniform stress distribution in the stiffened panels, a unique dynamic technique has been implemented to account for the stability performance by employing two sets of boundary conditions. The study demonstrates that maintaining stiffener eccentricity (e_{st}) within the range of 2.0 to 3.0 notably improves buckling strength depending on the type of edge loads.

Keywords


Stiffened laminates, non-uniform edge load, buckling, finite element method, heterosis element.

Graphical Abstract:



Received March 11, 2024. In revised form April 1, 2024. Accepted June 21, 2024. Available online June 28, 2024.

<https://doi.org/10.1590/1679-78258093>

 Latin American Journal of Solids and Structures. ISSN 1679-7825. Copyright © 2024. This is an Open Access article distributed under the terms of the [Creative Commons Attribution License](https://creativecommons.org/licenses/by/4.0/), which permits unrestricted use, distribution, and reproduction in any medium, provided the original work is properly cited.

1 INTRODUCTION

Fiber reinforced composites are frequently employed as subordinate elements within structural systems across a wide spectrum of engineering domains. Nonetheless, they encounter highly complex loading conditions throughout their operational lifespan. The non-uniform in-plane edge load stands out as the primary factor that notably modifies the natural vibration response of structural components. Indeed, a scenario may arise wherein the natural frequency of the structural element diminishes to zero under a specific intensity of in-plane load, precipitating instability within the components. Consequently, premature failure of laminated composites becomes a distinct possibility, especially for the structural element with openings. Moreover, to strengthen the stability of the panel, reinforcements such as beams or stiffeners are very much required, especially when subjected to diverse environmental conditions. The stiffened panel demonstrates commendable efficiency in enhancing structural strength without imposing a significant burden on the structure's weight. Hence, acquiring a comprehensive understanding of the stability characteristics of stiffened composite structures under diverse non-uniform edge loads is very much essential for evaluating their structural performance, a matter that has gained considerable attention in recent years.

In order to investigate the buckling behaviour of stiffened laminated composite panels, it is crucial to first understand how these panels behave without stiffeners. In this context, over the past few years, many researchers have delved into the buckling capacity of panels with and without openings under uniform edge loads (Shanmugam et al., 1999; Altunsaray and Bayer 2014; Nguyen et al., 2024). Typically, these panels are integral parts of complex structures, and their interaction with adjacent components may lead to non-uniform loading. Hence, for a comprehensive analysis, it is imperative to consider non-uniform loads. Some researchers have investigated the buckling behavior of unreinforced perforated and non perforated panels under non-uniform edge loads (Ghannadpour et al., 2006; Rajanna et al., 2016a; Subash Chandra et al., 2020; Muddappa et al., 2021; Hirannaiah et al., 2023; Swaminathan et al., 2023; Yathish Muddappa et al., 2023a).

The previous discussions primarily focused on panels without stiffeners, yet panels with stiffeners are prevalent in various practical applications, such as aircraft fuselages and wings, ship hulls and decks, offshore drilling rigs, pressure vessels, roofing units, and rocket launching pedestals. Timoshenko and Gere (1961) examined the buckling behavior of rectangular stiffened panels with longitudinal and transverse ribs. Mukhopadhyay and Mukherjee (1990) conducted stability analysis of reinforced plates using a semi-analytical finite difference method, highlighting the significant improvement in buckling strength with longitudinal stiffeners compared to lateral ones. Jaunky et al., (1996) investigated grid-reinforced composite panel stability, considering skin-stiffener interaction effects. Satish Kumar and Mukhopadhyay (1999) developed a new finite element method incorporating triangular compressive and shear loads, while Huang et al., (2015) demonstrated the superiority of grid-type stiffeners over bi-directional ones under bi-directional loading. Similarly, Zhao and Kapania (2016) employed an efficient finite element method to examine the buckling capacity of the reinforced panel. They introduced displacement continuity conditions at the panel-stiffener interface to evade re-meshing. Sadamoto et al., (2017) examined the buckling performance of stiffened panel by employing an efficient Galerkin mesh-free flat shell formulation. To avoid the shear-locking problem, the stiffness matrix was integrated employing stabilized conforming nodal integration (SCNI). Later, Rajanna et al., (2018) studied reinforced perforated panel buckling under uniform edge loads, though only ring stiffeners were considered, providing stress concentration relief but not significant buckling strength enhancement. Deng et al., (2019) introduced a method for investigating local and overall buckling modes of reinforced panels, allowing stiffener placement anywhere within the plate. Despite the practical importance of non-uniform edge loads, technical literature on the subject is limited, likely due to the analysis complexity. Rajanna et al., (2016b) investigated the effect of partial edge loads on the buckling characteristics of stiffened laminated composite panels. The effect of various non-uniform edge loads such as partial load from one edge, partial load from both edges and load from the central portion of panel have been considered in their study. Chandra et al. (2022) developed finite element formulations for predicting the stability of laminated composite panels with ring stiffener around the cutout under non-uniform edge loads. They tackled displacement compatibility at the interface between the panel and stiffeners utilizing the first-order shear deformation theory. Even though stress concentration decreases, the absence of longitudinal stiffeners alongside the ring stiffener did not notably enhance buckling strength.

In order to enhance buckling strength, it is essential to distribute stiffeners evenly across the panel rather than concentrating them solely around the cutout. Exploring number of stiffeners under non-uniform edge loads becomes crucial for increasing strength. Existing literature shows insufficient information on this aspect. Kalgutkar et al., (2023) recently investigated the impact of different elliptical cutout orientations on stiffened panel stability under non-uniform edge loads using ABAQUS FE software. Their study incorporated longitudinal stiffeners away from the cutout, yet these failed to mitigate stress concentration at the cutout edges. Similarly, Yathish Muddappa et al., (2023b) analyzed the

buckling behavior of perforated fiber metal laminates reinforced with ring flat stiffeners around the cutout under uniform and non-uniform edge loads. While stress concentration reduced, but not notably enhance buckling strength due to the absence of longitudinal stiffeners alongside the ring stiffener. Zeybek and Özkılıç (2023) demonstrated that appropriately sized intermediate ring stiffeners positioned at the cylindrical shell midpoint effectively stabilize structures, particularly in windy conditions, through analytical and numerical analyses.

Existing literature predominantly covers the buckling behavior of panels with or without cutouts under uniformly distributed edge loads, with limited research on non-uniform edge load effects. Few studies focus on the stability of perforated reinforced panels under non-uniform edge loads. On the contrary, the stiffened panel under the action of non-uniform edge load is scarcely addressed in the literature. This investigation examines the influence of various non-uniform in-plane edge loads, stiffener eccentricities, cutout sizes and ply-orientations on laminated stiffened panel buckling behavior.

2 THEORY AND FINITE ELEMENT FORMULATION

The mathematical formulation for analyzing the buckling characteristics of stiffened laminated composite panels using finite element techniques involves considering a panel of dimensions $a \times b \times h$, with an attached stiffener of cross-section $b_s \times d_s$. A schematic diagram of the stiffened panel in the cartesian coordinate system (x - y - z) is presented in figure 1(a), figure 1(b) displays a mesh pattern of atypical panel featuring a circular cutout at the center and figure 1(c) represents a typical panel under the action of a typical in-plane edge load. The mesh pattern is designed to have a finer resolution near the perforation region while minimizing edge skewness. Moreover, the outer region of the panel maintains a rectangular mesh with an aspect ratio close to 1. Additionally, figure 2 illustrates seven types of non-uniform edge loads, including five linear variations (figures 2a to 2e) described by the loading function, $P_y = P_0 (1 - \alpha y/b)$, along with sinusoidal and inverse sinusoidal edge loads shown in figures 2 (f) and 2 (g), respectively. Here, P_0 represents the maximum intensity of load per unit length and α is the load-defining factor to obtain different kinds of loading patterns as shown in figure 2. For instance, $\alpha = 0$ defines uniformly distributed edge load (figure 2 (a)) and $\alpha = 2.0$ defines pure in-plane bending (figure 2 (e)). By varying the value of α , one can obtain different patterns of linearly varying edge loads as shown in figure 2 (a) – (e). The analysis also explores six different eccentric stiffener patterns depicted in figure 3.

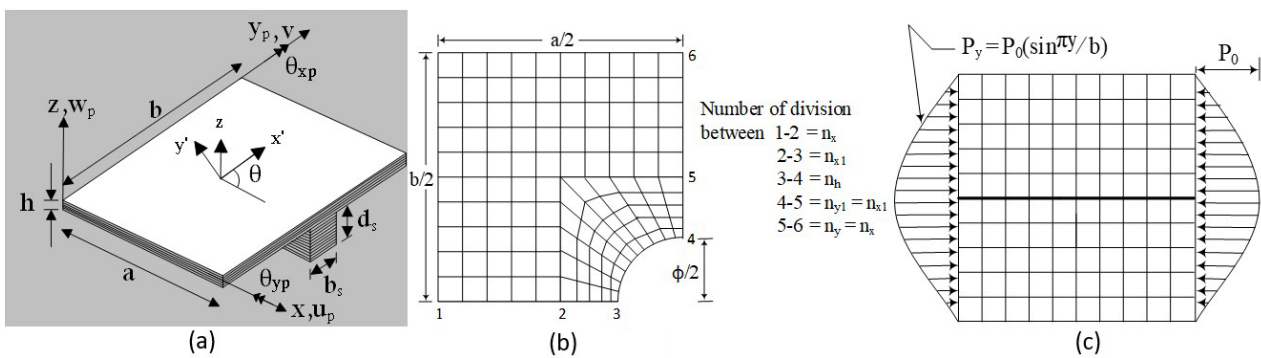


Figure 1 (a) Conceptual model of a stiffened laminated panel (b) Detailed mesh pattern over a quarter panel (c) Typical panel under a typical edge load for the case of sinusoidal edge load.

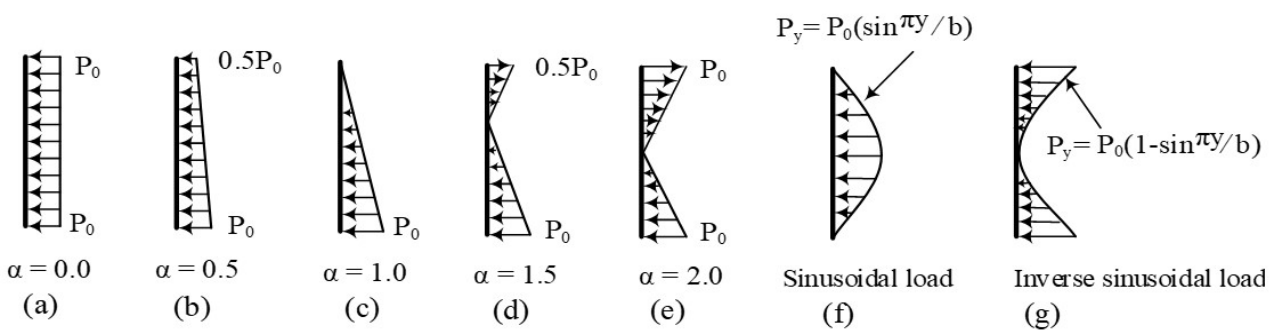


Figure 2 Panel with different loading patterns.

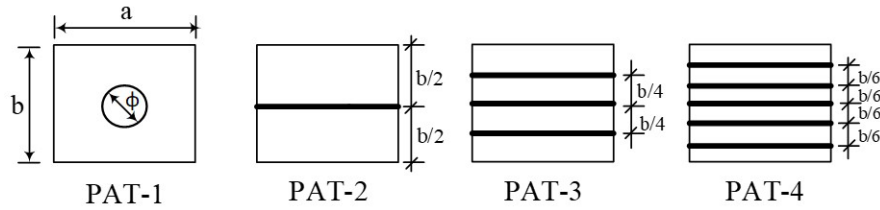


Figure 3 Different typical stiffener configurations.

2.1 Governing equations

The equation of motion for the stiffened laminated composite panel applied with non-uniform in-plane edge loading condition (figure 2) can be expressed as,

$$[M]\{\ddot{q}\} + \left([K] - P_0 [K_G] \right) \{q\} = \{0\} \tag{1}$$

where [M], [K] and [K_G] are the consistent mass matrix, elastic stiffness matrix and geometric stiffness matrix due to in-plane load, respectively. Equation (1) can be simplified for buckling and vibration problems as given below:

Buckling problem: When $\{\ddot{q}\}=0$, Eq. (1) reduces to a static case as,

$$[K]\{q\} - P_{cr} [K_G]\{q\} = \{0\} \tag{2}$$

Vibration problem: When the structural component vibrates harmonically under the action of in-plane edge load, Eq. (1) becomes,

$$[K]\{q\} - P_0 [K_G]\{q\} - \omega^2 [M]\{q\} = \{0\}. \tag{3}$$

In the above equation (Eq. 3), when P₀ approaches zero, the equation describes a free vibration problem without an in-plane load. If P₀ is nonzero, the equation still describes a free vibration problem but with the influence of an in-plane load. At a specific value of P₀ in Equation (3), the frequency's square (ω²) reaches zero, indicating the critical buckling load. Determining the buckling load using this dynamic approach proves highly convenient as it circumvents singularity issues inherent in eigenvalue solvers used in static analysis. This analytical method has been employed to ascertain critical loads for various scenarios discussed in this study.

2.2 Plate element formulation

The panel is discretized using a 9-noded heterosis plate element, as illustrated in figure 4. This element incorporates five degrees of freedom (u, v, w, θ_x, and θ_y) at all exterior nodes and four degrees of freedom (u, v, θ_x, and θ_y) at the interior node. The heterosis element, depicted in figure 4(a), is derived from both the eight-noded serendipity (figure 4(b)) and nine-noded Lagrange elements (figure 4(c)). The comprehensive formulation of the heterosis plate element along with its corresponding stiffness matrices has been extensively discussed by Rajanna et al. (2016b), and thus is not presented here to avoid repetition.

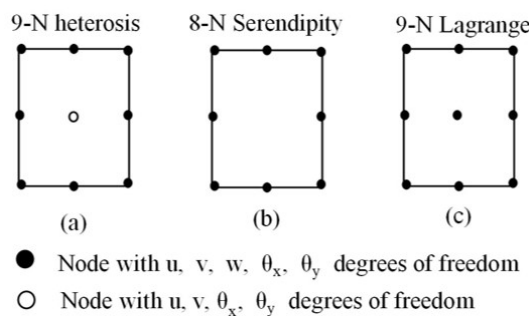


Figure 4 Different types of plate elements.

Using the Reissner–Mindlin hypothesis, the displacement field in terms of primary in-plane displacements (\bar{u}, \bar{v}) and transverse displacement (\bar{w}) with respect to mid-plane displacements (u, v, w) and rotations (θ_x, θ_y) at a point (x, y, z) by incorporating the shear deformation effect is expressed as, Ravi Kumar et al., (2005).

$$\{\bar{u}(x, y, z), \bar{v}(x, y, z), \bar{w}(x, y, z)\} = \{u(x, y), v(x, y), w(x, y)\} + z\{\theta_x(x, y), \theta_y(x, y), 0\} \tag{4}$$

Even though a linear analysis is performed in the current work, the initial stress stiffness is calculated by employing the Green–Lagrange strain displacement relation. As a result, Green–Lagrange’s strain displacement relation with reference to a plate element in Cartesian coordinate system is expressed as (Cook, 2007).

$$\left. \begin{aligned} \varepsilon_x &= \left(\frac{\partial \bar{u}}{\partial x} \right) + \frac{1}{2} \left(\frac{\partial u}{\partial x} \right)^2 + \frac{1}{2} \left(\frac{\partial v}{\partial x} \right)^2 + \frac{1}{2} \left(\frac{\partial w}{\partial x} \right)^2 + \frac{1}{2} z^2 \left[\left(\frac{\partial \theta_x}{\partial x} \right)^2 + \left(\frac{\partial \theta_y}{\partial x} \right)^2 \right] \\ \varepsilon_y &= \left(\frac{\partial \bar{v}}{\partial y} \right) + \frac{1}{2} \left(\frac{\partial u}{\partial y} \right)^2 + \frac{1}{2} \left(\frac{\partial v}{\partial y} \right)^2 + \frac{1}{2} \left(\frac{\partial w}{\partial y} \right)^2 + \frac{1}{2} z^2 \left[\left(\frac{\partial \theta_x}{\partial y} \right)^2 + \left(\frac{\partial \theta_y}{\partial y} \right)^2 \right] \\ \gamma_{xy} &= \left(\frac{\partial \bar{u}}{\partial y} + \frac{\partial \bar{v}}{\partial x} \right) + \frac{\partial u}{\partial x} \frac{\partial u}{\partial y} + \frac{\partial v}{\partial x} \frac{\partial v}{\partial y} + \left(\frac{\partial w}{\partial x} \right) \left(\frac{\partial w}{\partial y} \right) + z^2 \left[\frac{\partial \theta_x}{\partial x} \frac{\partial \theta_x}{\partial y} + \frac{\partial \theta_y}{\partial x} \frac{\partial \theta_y}{\partial y} \right] \end{aligned} \right\} \tag{5}$$

The strain-displacement equation, which is shown in Eq. (5) has two parts, i.e., linear strain and non-linear strains,

$$\{\varepsilon_{ij}\} = \{\varepsilon_{ij}^L\} + \{\varepsilon_{ij}^{NL}\} \tag{6}$$

The linear strain vector $\{\varepsilon_{ij}^L\}$ is used to derive elastic stiffness matrix, and the non-linear strain vector $\{\varepsilon_{ij}^{NL}\}$ is used for the geometric stiffness matrix (Bathe, 2006). The stress-strain relation for the laminated panel is given by (Reddy 1996)

$$\begin{Bmatrix} N_x \\ N_y \\ N_{xy} \\ M_x \\ M_y \\ M_{xy} \\ Q_{xz} \\ Q_{yz} \end{Bmatrix} = \begin{bmatrix} A_{11} & A_{12} & A_{16} & B_{11} & B_{12} & B_{16} & 0 & 0 \\ A_{12} & A_{22} & A_{26} & B_{12} & B_{22} & B_{26} & 0 & 0 \\ A_{16} & A_{26} & A_{66} & B_{16} & B_{26} & B_{66} & 0 & 0 \\ B_{11} & B_{12} & B_{16} & D_{11} & D_{12} & D_{16} & 0 & 0 \\ B_{12} & B_{22} & B_{26} & D_{12} & D_{22} & D_{26} & 0 & 0 \\ B_{16} & B_{26} & B_{66} & D_{16} & D_{26} & D_{66} & 0 & 0 \\ 0 & 0 & 0 & 0 & 0 & 0 & S_{44} & S_{45} \\ 0 & 0 & 0 & 0 & 0 & 0 & S_{45} & S_{55} \end{bmatrix} \begin{Bmatrix} u_{,x} \\ v_{,y} \\ u_{,y} + v_{,x} \\ \theta_{x,x} \\ \theta_{y,y} \\ \theta_{x,y} + \theta_{y,x} \\ w_{,x} + \theta_{xp} \\ w_{,y} + \theta_{yp} \end{Bmatrix} \tag{7}$$

The laminates constitutive coefficients in Eq. (7) are defined by,

$$(A_{ij}, B_{ij}, D_{ij}) = \sum_{k=1}^m \int_{z_{k-1}}^{z_k} (\bar{Q}_{ij})(1, z, z^2) dz \quad \text{for } i, j = 1, 2, 6 \tag{8}$$

whereas the shear component is indicated by $S_{ij} = \sum_{k=1}^m \int_{z_{k-1}}^{z_k} \kappa (\bar{Q}_{ij}) dz$ for $i, j = 4, 5$ (9)

in which m is the number of layers, κ is the shear correction factor, which is given by 5/6 (Lal and Saini, 2013).

The different participating element level matrices such as elastic stiffness matrix $[k_e]$, geometric stiffness matrix $[k_G]$ and consistent mass matrix $[m_e]$ have been derived using the corresponding energy expressions (Bathe, 2006):

$$[k_e] = \int_{-1}^1 \int_{-1}^1 [B]^T [D] [B] |J| d\xi d\eta \tag{10}$$

$$[k_G] = \int_{-1}^1 \int_{-1}^1 [B_G]^T [S] [B_G] |J| d\xi d\eta \tag{11}$$

$$[m_e] = \int_{-1}^{+1} \int_{-1}^{+1} [\bar{N}]^T [\bar{I}] [\bar{N}] |J| d\xi d\eta \tag{12}$$

in which, $[\bar{N}]$ is the shape function matrix and $[\bar{I}]$ is the inertia matrix consisting of I_1, I_2 and I_3 which are given by $(I_1, I_2, I_3) = \sum_{k=1}^m \int_{z_{k-1}}^{z_k} \rho_m(1, z, z^2) dz$. The global matrices are generated by assembling the corresponding element matrices and are stored in skyline form. The subspace iteration technique is adopted to solve the eigenvalue problems (Bathe, 2006).

2.3 Stiffener element formulation

figure 5 illustrates the standard geometry of a 3-noded isoparametric beam element with a width of b_s and a depth of d_s , using a positive set of coordinates. In this formulation, the stiffener is represented as a laminated beam, allowing it to be positioned in any arbitrary direction at an angle of ψ relative to the x-axis of the panel, as depicted in figure 5.

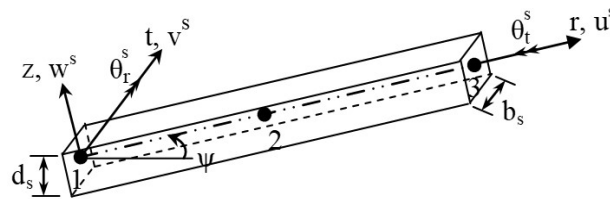


Figure 5 Arbitrarily oriented stiffener

The conventional beam model neglects the effect of lateral strains (Krishnaswamy et al., 1992). The elimination of lateral strains results in the loss of some stiffness coefficients and this type of analysis is restricted to cross-ply beams. In the present work, the constitutive relationship accounting for lateral strains (Kolli and Chandrashekhara, 1996), wherein the beam constitutive equation is derived from laminated plate equation, Eq. (7), by ignoring the stresses in the width or y-direction ($\sigma_y = \tau_{xy} = \tau_{yz} = 0$) but not the strains ($\epsilon_y \neq \gamma_{xy} \neq \gamma_{yz} \neq 0$).

The laminated constitutive equation for an arbitrary oriented stiffener can be written as,

$$\begin{Bmatrix} N_r \\ M_r \\ M_{rt} \\ Q_{rz} \end{Bmatrix} = \begin{bmatrix} \bar{A}_{11} & \bar{B}_{11} & \bar{B}_{16} & 0 \\ \bar{B}_{11} & \bar{D}_{11} & \bar{D}_{16} & 0 \\ \bar{B}_{16} & \bar{D}_{16} & \bar{D}_{66} & 0 \\ 0 & 0 & 0 & \bar{A}_{44} \end{bmatrix} \begin{Bmatrix} u_r \\ \theta_{r,r} \\ \theta_{t,r} \\ w_r + \theta_r \end{Bmatrix} \tag{13}$$

In abbreviated form, Eq. (13) is written as,

$$\begin{Bmatrix} \{N\} \\ \{Q\} \end{Bmatrix} = \begin{bmatrix} [D_b] & [0] \\ [0] & [D_s] \end{bmatrix} \begin{Bmatrix} \{\epsilon\} \\ \{\gamma\} \end{Bmatrix} \tag{14}$$

The term $[D_b]$ is given by, $[D_b] = \left[[a] - [b] * [c]^{-1} [b]^T \right]$ (15)

$$[a] = \begin{bmatrix} A_{11} & B_{11} & B_{16} \\ B_{11} & D_{11} & D_{16} \\ B_{16} & D_{16} & D_{66} \end{bmatrix}, \quad [b] = \begin{bmatrix} A_{12} & A_{16} & B_{12} \\ B_{12} & B_{16} & D_{12} \\ B_{26} & B_{66} & D_{26} \end{bmatrix} \quad \text{and} \quad [c] = \begin{bmatrix} A_{22} & A_{26} & B_{22} \\ A_{26} & A_{66} & B_{26} \\ B_{22} & B_{26} & D_{22} \end{bmatrix} \quad (16)$$

in which,

Further, $[D_s]$ is the shear constitutive relations, which is derived as,

$$[D_s] = \bar{A}_{44} (w_{,x} + \theta_x) \quad (17)$$

in which

$$\bar{A}_{44} = \left(A_{44} - \frac{A_{45}A_{45}}{A_{55}} \right) \quad (18)$$

Using Green-Lagrange's strain-displacement expression, the linear strain-displacement matrix $[B]$ and the non-linear strain-displacement matrix $[B_G]$ have been worked out. Similarly, the corresponding elastic stiffness matrix $[k_e]$, geometric stiffness matrix $[k_G]$ and mass matrix $[m]$ of the stiffener element may be expressed as follows:

$$[k_{es}] = b_s \int_{-1}^{+1} [T_e]^T [T_o]^T [B_s]^T [D_s] [B_s] [T_o] [T_e] |J_s| d\xi \quad (19)$$

$$[k_{Gs}] = b_s \int_{-1}^{+1} [T_e]^T [T_o]^T [B_{Gs}]^T [S_s] [B_{Gs}] [T_o] [T_e] |J_s| d\xi \quad (20)$$

$$[m_s] = b_s \int_{-1}^{+1} [T_e]^T [T_o]^T [\bar{N}_s]^T [\bar{I}_s] [\bar{N}_s] [T_o] [T_e] |J_s| d\xi \quad (21)$$

where $[T_e]$ and $[T_o]$ are transformation matrices, in which $[T_e]$ takes care of the eccentricity of the stiffener and $[T_o]$ takes care of arbitrary orientation of the stiffener, Rajanna et al. (2018).

3 RESULTS AND DISCUSSION

The analysis investigates the buckling behavior of stiffened panels under various non-uniform edge-loading conditions. The study focuses exclusively on eccentric stiffeners, which are attached to the bottom face of the plate. The panel's thickness-to-width ratio (h/b) is set at 0.01, and unless otherwise specified, the stiffener width is equal to the panel thickness. The material properties for both the panel and the stiffeners are $E_1 = 25$, $E_{22} = 1.0$, $G_{12} = G_{13} = 0.50$, $G_{23} = 0.20$, and $\nu_{12} = 0.25$ unless specified otherwise. Boundary conditions are defined using the notations S (simply supported), C (clamped), and F (free), consistent with those outlined by Rajanna et al. (2016a).

The vibration frequency and the critical loads are presented in non-dimensional form as follows [Reddy and Phan (1985)] (Table 1).

Table 1: Non-dimensional parameters

No.	Parameter	Stiffened/unstiffened panels	
		Isotropic	Composite
1	Non-dimensional frequencies ($\bar{\omega}$)	$\omega b^2 \sqrt{\rho h / D}$	$\omega b^2 \sqrt{\rho / E_{22} h^2}$
2	Non-dimensional buckling load (ν_{cr})	$P_{cr} b^2 / D$	$P_{cr} b^2 / E_{22} h^3$
where $D = Eh^3/12(1-\nu^2)$, ω and P_{cr} are the absolute frequencies and absolute critical loads, respectively.			

3.1 Comparative studies—panel without cutout

To verify the accuracy of the computed stiffness and mass matrices, the free vibration response of a square laminated panel without a cutout is predicted. This prediction is carried out using three different types of elements: the

9-noded heterosis element (9-NHE), 9-noded Lagrange element (9-NLE), and 8-noded serendipity element (8-NSE). The results are compared with the closed-form solutions (CFS) provided by Reddy and Phan (1985), as presented in Table 2. Similarly, to assess the accuracy of the geometric stiffness matrix, buckling analysis is conducted on a cross-ply laminated square panel subjected to various types of non-uniform edge loads. This analysis utilizes the same three types of elements for different h/b ratios. The results, along with the closed-form solutions of Zhong and Gu (2007), are tabulated in Table 3. While all elements yield satisfactory results in both vibration and buckling analyses, the heterosis element demonstrates better accuracy. Consequently, the heterosis element is utilized for the remaining of the work.

Table 2: Non-dimensional frequencies (ω) of SSSS edged angle-ply square panel;
 $E_{11}/E_{22} = 40, G_{12} = G_{13} = 0.6E_{22}, G_{23} = 0.5E_{22}$ and $\nu_{12} = 0.25$.

b/h	2 layers (45/-45)				8 layers (45/-45/45...)			
	Present results			(Reddy and Phan 1985)	Present results			(Reddy and Phan 1985)
	9-NHE	9-NLE	8-NSE		9-NHE	9-NLE	8-NSE	
5	10.335	10.244	10.243	10.335	12.892	12.863	12.862	12.892
10	13.044	12.975	12.975	13.044	19.289	19.235	19.235	19.289
20	14.179	14.154	14.153	14.179	23.259	23.225	23.225	23.259
25	14.338	14.322	14.321	14.338	23.924	23.899	23.899	23.924
50	14.561	14.557	14.556	14.561	24.909	24.902	24.901	24.909
100	14.618	14.617	14.617	14.618	25.176	25.174	25.174	25.176

Table 3: Comparison of γ_{cr} for cross-ply square panels (0/90/0) under linearly varying loads;
 $E_1/E_2 = 40, G_{12} = G_{13} = 0.6E_{22}, G_{23} = 0.5E_2$ and $\nu_{12} = 0.25$.

Load pattern (α)	Source	h/b = 0.01	h/b = 0.05	h/b = 0.1
0.5	Zhong and Gu (2007)	47.267	41.075	29.432
	9–Heterosis	47.261	40.939	29.228
	9–Lagrangian	47.259	40.930	29.225
	8–Serendipity	47.256	40.921	29.120
1.0	Zhong and Gu (2007)	64.982	56.705	40.999
	9–Heterosis	64.975	56.486	40.525
	9–Lagrangian	64.962	56.478	40.514
	8–Serendipity	64.960	56.457	40.500
1.5	Zhong and Gu (2007)	91.374	80.336	47.708
	9–Heterosis	91.355	79.989	48.300
	9–Lagrangian	91.338	79.957	48.291
	8–Serendipity	91.331	79.930	48.285
2.0	Zhong and Gu (2007)	129.785	114.837	47.872
	9–Heterosis	129.758	114.167	48.720
	9–Lagrangian	129.730	114.152	48.660
	8–Serendipity	129.725	113.980	48.514

3.2 Comparative studies– unstiffened panel with cutouts

To broaden the comparative study, the validation of the panel with various cutout sizes is extended to include the analysis of buckling issues under uniformly distributed edge loads. Critical buckling loads are assessed for panels comprised of 8-layered (0/90)_{2s} and 40-layered (45/-45/0/90)_{5s} laminates using the heterosis element. The validation encompasses cutouts of six different sizes. Results are presented in Table 4, alongside those obtained using the FE package ANSYS and findings from similar studies reported by other researchers (Jain and Kumar, 2004; Ghannadpour et al., 2006). The results obtained using the FE package ANSYS are enclosed in parentheses. A notable agreement is observed between the outcomes of the present study and those from existing literature and the FE package ANSYS.

Table 4: Non-dimensional buckling load parameters (γ_{cr}) for simply supported square laminates with central circular cutout under uniform edge loads; $E_{11} = 130.0$ GPa, $E_{22} = 10.0$ GPa and $\nu_{12} = 0.35$, $G_{12} = G_{13} = 5.0$ GPa, $G_{23} = 3.4$ GPa.

ϕ/b	40-layers (45/-45/0/90) _{5S} , b/h = 75		8-layers (0/90) _{2S} , b/h = 100	
	Present	Jain and Kumar (2004)	Present	Ghannadpour et al., (2006)
0.0	19.16 (19.16)	19.23	13.82 (13.83)	13.79
0.1	18.41 (18.43)	18.56	12.83 (12.84)	12.80
0.2	16.94 (16.96)	17.10	10.84 (10.85)	10.82
0.3	15.40 (15.41)	15.30	8.98 (08.99)	8.97
0.4	14.63 (14.63)	14.63	7.52 (07.52)	7.51
0.5	13.96 (13.97)	13.84	6.40 (06.40)	6.39

3.3 Comparative studies– stiffened panel

Additionally, the buckling behavior of a simply supported panel with a central single stiffener under uniformly distributed edge load across width b is investigated for varying bending rigidity of the stiffener. The parameter δ ranges from 0.05 to 0.20, while β varies from 5 to 15. Results, presented in Table 5 in non-dimensional form as $\gamma_{cr} = P_{cr}b^2/(\pi^2D)$, are compared with classical solutions of Timoshenko and Gere (1961), numerical solutions from Mukhopadhyay and Mukherjee (1990), and Hamedani and Ranji (2013). Across all cases, the present results align well with those in existing literature, affirming the accuracy of both the geometric stiffness matrix for the plate and the stiffeners.

Table 5: Validation of non-dimensional critical loads for a simply supported square stiffened panel.

β	η	Non-dimensional buckling load					
		Neglecting T and e			Considering T and e		
		Timoshenko and Gere (1961)	Mukhopadhyay and Mukherjee (1990)	Hamedani and Ranji (2013)	Present (heterosis)	Hamedani and Ranji (2013)	Present (heterosis)
5	0.05	12.00	11.72	11.80	11.80	11.91	11.86
	0.10	11.10	10.93	10.98	10.98	11.09	11.27
	0.20	9.72	9.70	9.69	9.69	9.86	10.01
10	0.05	16.00	16.00	15.97	15.97	18.16	17.91
	0.10	16.00	16.00	15.97	15.97	16.97	17.20
	0.20	15.80	15.44	15.67	15.67	15.04	15.77
15	0.05	16.00	16.00	15.97	15.97	20.41	20.30
	0.10	16.00	16.00	15.97	15.97	20.41	20.33
	0.20	16.00	16.00	15.97	15.97	19.36	20.33

T and e = Torsional rigidity and eccentricity of the stiffener

3.4 Stability analysis of perforated composite laminates with various patterns of stiffener subjected to diverse non-uniform edge loadings.

In many scenarios, stiffened panels undergo diverse forms of non-uniform edge loading, leading to uneven stress distribution within the panel. This non-uniform stress distribution significantly impacts the stability characteristics of the stiffened panels. Additionally, the presence of a cutout within the panel can induce local buckling, potentially influencing global buckling behavior and causing an overall decline in stiffness, the extent of which relies on the size and shape of the cutout. The reduction in stiffness due to cutouts can be mitigated by selecting an appropriate number of stiffeners and its eccentricity. Therefore, it is imperative to conduct a comprehensive investigation into the factors influencing the stability attributes of the structure. Thus, this study delves into the impact of various stiffeners and their eccentricity on the stability characteristics of composite laminates under diverse non-uniform edge loads. The assorted types of non-uniform loading and stiffener patterns considered for the case study are depicted in figure 2 and figure 3, respectively. An eight-layered symmetric cross-ply (0/90)_{2S} and angle-ply (± 45)_{2S} laminated configurations are employed for the panel, with the ply-orientation of the stiffener consistently parallel to its axis, irrespective of its orientation. Moreover, the thickness-to-width ratio of the panel (h/b) is set at 0.01, and the stiffener width matches the panel thickness unless stated otherwise. Various parametric analyses are conducted in the subsequent subsections.

3.4.1 Effect of various non-uniform edge loads on different cutout sizes.

The study investigates the impact of various non-uniform in-plane edge loads on the buckling behavior of square panels with SSSS edges, using cross-ply and angle-ply laminate configurations and the results are plotted in figures 6(a) and 6(b) respectively. Figure 6(a) reveals that the buckling resistance of the panel declines as the cutout size increases, regardless of the loading patterns. Conversely, Figure 6(b) demonstrates a different behavior with the angle-ply laminate scheme, showing higher buckling resistance. Although the buckling resistance still decreases with the cutout size, an increase is observed for cutout sizes $\phi/b \geq 0.5$ in pure in-plane bending and $\phi/b \geq 0.3$ under inverse sinusoidal loading. This phenomenon is likely due to the stress redistribution from the cutout area to the stiffer regions at the panel edges. This redistribution is more significant under specific loading conditions, particularly with pure in-plane bending ($\alpha = 2.0$) and inverse sinusoidal edge loads. Additionally, the figures show that for a given cutout size, significantly higher buckling resistance occurs with pure in-plane bending ($\alpha = 2.0$) and inverse sinusoidal edge loads, while it is negligible for uniformly distributed and sinusoidal edge loads. The increased buckling resistance in pure bending ($\alpha = 2.0$) can be attributed to tensile stresses that counteract the loss of bending stiffness due to the cutout. Similarly, the higher buckling resistance under inverse sinusoidal edge loads may result from stress concentration towards the panel edges, where stiffness is considerably greater. In contrast, sinusoidal and uniformly distributed edge loads tend to concentrate the majority of stresses toward the central portion of the panel, resulting in lower buckling resistance.

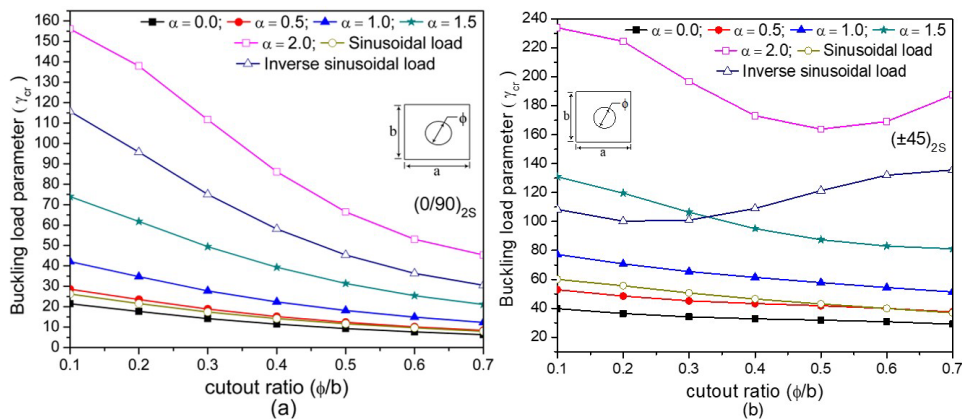


Figure 6 Variation of γ_{cr} with different cutout sizes (ϕ/b) for (a) $(0/90)_{2s}$ and (b) $(\pm 45)_{2s}$ stacking panel.

3.4.2 Effect of stiffener eccentricities on various non-uniform edge loads

In this section, the buckling behavior of a square panel with SSSS edges, featuring a centrally placed stiffener has been examined. The investigation is mainly focused on the effect of stiffener eccentricities (e_{st}) under various loading conditions. The panel configurations include a cross-ply scheme $(0/90)_{2s}$ and an angle-ply scheme $(\pm 45^\circ)_{2s}$, with results shown in Figures 7(a) and 7(b), respectively. The stiffener's fiber orientation remains parallel to its axis, and the panel's thickness-to-width ratio (h/b) is 0.01, with the stiffener's width matching the panel's thickness. A stiffener eccentricity of $e_{st} = 0.5$ represents a panel without a stiffener, corresponding to a stiffener depth of $d_{st} = 0.0$.

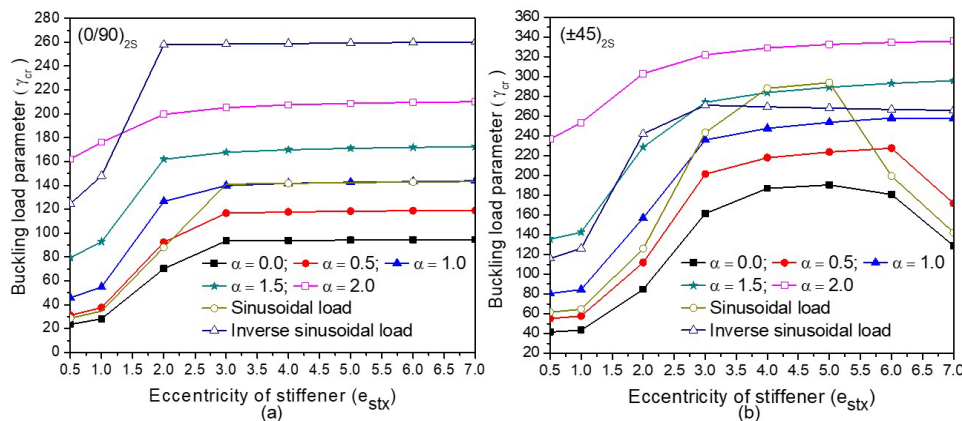


Figure 7 Variation of γ_{cr} with stiffener eccentricities (e_{st}) for (a) $(0/90)_{2s}$ and (b) $(\pm 45)_{2s}$ stacking SSSS edged stiffened panel under various non-uniform edge loads.

Figure 7(a) demonstrates that the buckling resistance of the stiffened panel increases sharply with increasing stiffener eccentricity (e_{st}) upto around 2.0 to 3.0, depending on the loading conditions, and then stabilizes regardless of further increase in the stiffener eccentricities (e_{st}). IT is also noticed that the panel subjected to pure bending ($\alpha = 2.0$) and inverse sinusoidal edge loads exhibit higher buckling resistance, while those under uniformly distributed edge load and sinusoidal edge load show the least buckling resistance.

In contrast, Figure 7(b) reveals a different behavior for the angle-ply laminate scheme, characterized by generally higher buckling resistance. Here, the buckling resistance of the stiffened panel increases with stiffener eccentricities (e_{st}) across most loading conditions, except for panels with uniformly distributed loads (UDL, $\alpha = 0.0$), linearly varying edge loads, $\alpha = 0.5$, and sinusoidal edge loads. In these cases, the buckling resistance increases upto a certain point of stiffener eccentricity (e_{st}) and then declining as stiffener eccentricity continues to increase. This trend may be due to a reduction in the stiffener's torsional stiffness. In both configurations, the stiffened panel with pure in-plane bending exhibits the highest buckling resistance, while those with uniformly distributed edge loads show the least.

3.4.3 Effect of number of stiffeners on various loading cases.

This section examines the impact of the number of stiffeners (n_s) on the buckling behavior of panels under various non-uniform loading conditions, using cross-ply $(0/90)_{2s}$ and angle-ply $(\pm 45)_{2s}$ lamination schemes. The results are shown in figures 8(a) and 8(b). The stiffener's ply orientation is always parallel to its axis, and the panel has a thickness-to-width ratio (h/b) of 0.01, with the stiffener's width matching the panel's thickness. Stiffeners are equidistantly spaced as illustrated in Figure 3.

Figures 8(a) and 8(b) reveal that the buckling resistance of the panel consistently increases with the number of stiffeners, regardless of the loading conditions. Additionally, for a given number of stiffeners, the stiffened panel subjected to pure bending and inverse sinusoidal edge load demonstrates the highest buckling resistance, while the panel under uniformly distributed edge load exhibits the least buckling resistance. This trend is observed in both cross-ply and angle-ply laminate schemes. However, panels with the cross-ply laminate scheme show higher buckling resistance compared to those with the angle-ply scheme.

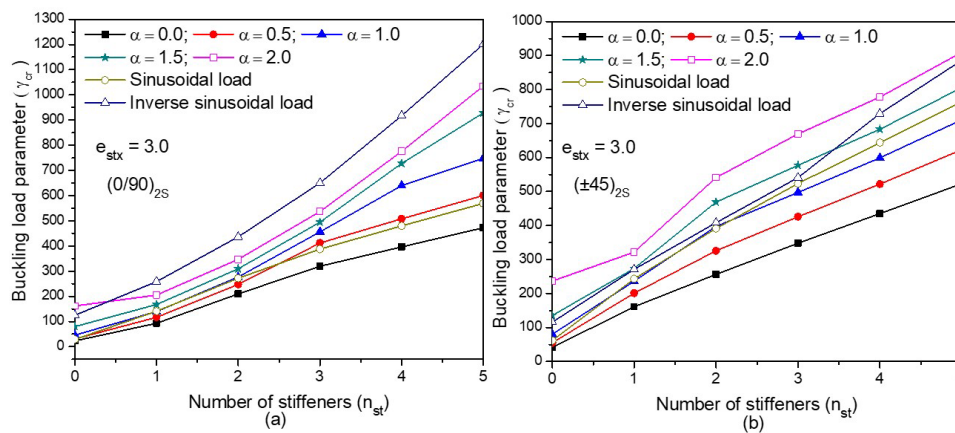


Figure 8 Variation of γ_{cr} with equispaced number of stiffeners (n_{st}) for (a) $(0/90)_{2s}$ and (b) $(\pm 45)_{2s}$ stacking sequences of SSSS edged square stiffened panels.

3.4.4 Effect of panel aspect ratios on different loading cases.

Figures 9(a) and 9(b) illustrate the effect of different panel aspect ratios on the buckling behavior of a panel with a centrally placed stiffener, considering both cross-ply and angle-ply lamination schemes. The stiffener eccentricity (e_{st}) is fixed at 3.0. In Figure 9(a), the panel's buckling resistance remains relatively constant across all panel aspect ratios, irrespective of the loading conditions. For any given panel aspect ratio, the stiffened panel subjected to inverse sinusoidal edge load exhibits the highest buckling resistance, while the panel under uniformly distributed edge load shows the least buckling resistance when compared to other loading scenarios. This indicates a general stability in buckling performance for cross-ply laminates regardless of the aspect ratio changes.

Conversely, Figure 9(b) reveals a different trend for panels with an angle-ply laminate scheme. Here, the buckling resistance of the stiffened panel consistently decreases as the panel aspect ratio increases, regardless of the loading conditions. However, exceptions are noted for panels under in-plane bending loads, specifically with $\alpha = 2.0$ and $\alpha = 1.5$, where the buckling resistance remains constant across all panel aspect ratios. This suggests that the angle-ply laminate

scheme is more sensitive to changes in aspect ratio, leading to a decline in buckling performance except in specific loading cases where the resistance is stabilized by the in-plane bending loads.

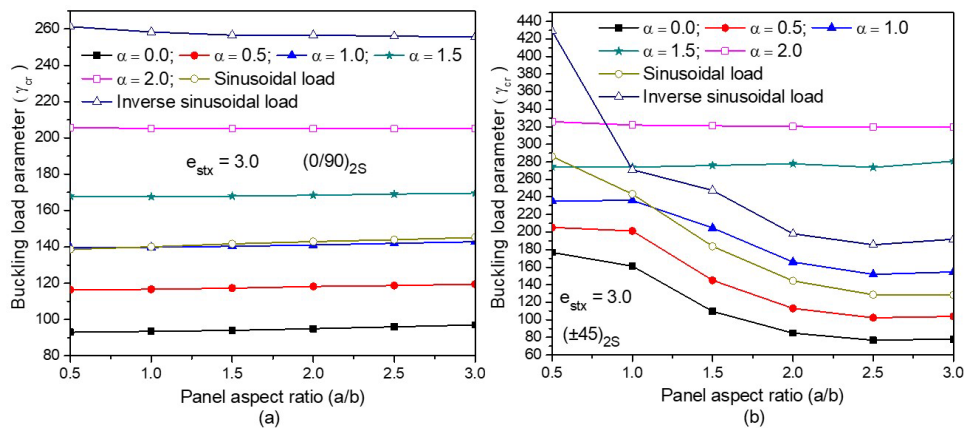


Figure 9 Variation of γ_{cr} with different panel aspect ratios by considering (a) $(0/90)_{2s}$ and (b) $(\pm 45)_{2s}$ stacking sequences of SSSS edged square panels.

4 CONCLUSION

The results obtained from the analysis of a panel's stability under various non-uniform edge loadings and different stiffener patterns are summarized below:

1. Among all loading types, the panel exhibits highest buckling resistance under pure in-plane bending ($\alpha = 2.0$) as well as inverse sinusoidal edge loads and lowest under uniform edge loads ($\alpha = 0.0$).
2. In the case of a cross-ply laminate scheme, the buckling resistance of the panel increases with the rise in stiffener eccentricity (e_{st}) up to a certain point, after which it remains constant regardless of the loading cases.
3. For angle-ply laminates, the buckling resistance sharply increases with stiffener eccentricity (e_{st}) up to a certain point and then levels off, except under uniformly distributed loads ($\alpha = 0.0$), linearly varying edge loads ($\alpha = 0.5$), and sinusoidal edge loads, where it declines after reaching a certain eccentricity.
4. The buckling resistance of the panel increases with the number of stiffeners, regardless of the loading cases. However, there is an abrupt increase in resistance in the case of pure bending ($\alpha = 0.5$) and inverse sinusoidal edge loads.
5. For cross-ply laminates, the panel's buckling resistance remains constant across all aspect ratios, regardless of loading conditions. In contrast, for angle-ply laminates, buckling resistance consistently decreases with aspect ratio, except under in-plane bending loads ($\alpha = 2.0$ and $\alpha = 1.5$), where it remains constant.

Author's Contributions: Methodology, Investigation, Validation, Writing Original Draft by Sasha azimi and Asha K; Conceptualization, Writing - Reviewing & Editing, Supervision by Rajanna T, Akshay Prakash Kalgutkar & Ravindra P.K.

Editor: Marco L. Bittencourt

References

- Altunsaray, E., Bayer, I., (2014). Buckling of symmetrically laminated quasi-isotropic thin rectangular plates. *Steel and Composite Structures*, 17(3):305-320. <https://doi.org/10.12989/scs.2014.17.3.305>.
- Bathe, K.J., (2006). *Finite element procedures*, Prentice Hall, Pearson Education, Inc.
- Chandra, K.S., Rajanna, T., Rao, K.V., (2022). Thermal buckling analysis of stiffened composite cutout panels. In *Recent Trends in Construction Technology and Management*, 935-948. https://link.springer.com/chapter/10.1007/978-981-19-2145-2_69.
- Cook, R.D., (2007). *Concepts and applications of finite element analysis*, John Wiley & sons.

- Deng, J., Wang, X., Yuan, Z., Zhou, G., (2019). An efficient technique for simultaneous local and overall buckling analysis of stiffened panels, *Advances in Engineering Software*, 131: 36-47. <https://doi.org/10.1016/j.advengsoft.2019.03.002>.
- Ghannadpour, S.A.M., Najafi, A., Mohammadi, B., (2006). On the buckling behavior of cross-ply laminated composite plates due to circular/elliptical cutouts. *Composite Structures*, 75(1):3-6. <https://doi.org/10.1016/j.compstruct.2006.04.071>.
- Hamedani, S.J., Ranji, A.R., (2013). Buckling analysis of stiffened plates subjected to non-uniform biaxial compressive loads using conventional and super finite elements. *Thin-Walled Structures*, 64:41-49. <https://doi.org/10.1016/j.tws.2012.12.004>.
- Hirannaiah, S., Swaminathan, K., Rajanna, T., (2023). Thermo-mechanical vibration and buckling analysis of porous FG sandwich plates with geometric discontinuity based on physical neutral surface." *Mechanics of Advanced Materials and Structures*, 1-25. <https://doi.org/10.1080/15376494.2023.2220493>.
- Huang, L., Sheikh, A.H., Ng, C.T., Griffith, M.C., (2015). An efficient finite element model for buckling analysis of grid stiffened laminated composite plates. *Composite Structures*, 122: 41-50. <https://doi.org/10.1016/j.compstruct.2014.11.039>.
- Jain, P., Kumar, A., (2004). Postbuckling response of square laminates with a central circular/elliptical cutout. *Composite Structures*, 65(2):179-185. <https://doi.org/10.1016/j.compstruct.2003.10.014>.
- Jaunky, N., Knight, N.F., Ambur, D.R., (1996), Formulation of an improved smeared stiffener theory for buckling analysis of grid-stiffened composite panels. *Composites Part B: Engineering*, 27(5):519-526. [https://doi.org/10.1016/1359-8368\(96\)00032-7](https://doi.org/10.1016/1359-8368(96)00032-7).
- Kalgutkar, A. P., Banerjee, S., Rajanna, T., (2023). Effect of elliptical cutouts on buckling and vibration characteristics of stiffened composite panels under non-uniform edge loads. *Mechanics Based Design of Structures and Machines*, 51(9):5340-5354. <https://doi.org/10.1080/15397734.2021.1999266>.
- Kolli, M., Chandrashekhara, K., (1996). Finite element analysis of stiffened laminated plates under transverse loading. *Composites Science and Technology*, 56(12):1355-1361. [https://doi.org/10.1016/S0266-3538\(96\)00086-3](https://doi.org/10.1016/S0266-3538(96)00086-3).
- Krishnaswamy, S., Chandrashekhara, K., Wu, W.Z.B., (1992). Analytical solutions to vibration of generally layered composite beams. *Journal of Sound and Vibration*, 159(1):85-99. [https://doi.org/10.1016/0022-460X\(92\)90452-4](https://doi.org/10.1016/0022-460X(92)90452-4).
- Lal, R., Saini, R., (2013). Buckling and vibration of non-homogeneous rectangular plates subjected to linearly varying in-plane force. *Shock and Vibration*, 20:879-894. <https://doi.org/10.3233/SAV-130791>.
- Muddappa, P.P.Y., Rajanna, T., Giridhara, G., (2021). Effects of different interlaminar hybridization and localized edge loads on the vibration and buckling behavior of fiber metal composite laminates. *Composites Part C: Open Access*, 4(1):100084-1-13. <https://doi.org/10.1016/j.jcomc.2020.100084>.
- Mukhopadhyay, M., Mukherjee, A., (1990). Finite element buckling analysis of stiffened plates. *Computers and Structures*, 34(6): 795-803. [https://doi.org/10.1016/0045-7949\(90\)90350-B](https://doi.org/10.1016/0045-7949(90)90350-B).
- Nguyen, T.T., Le, T.S., Tran, T.T., Pham, Q.H., (2024). Buckling analysis of functionally graded porous variable thickness plates resting on Pasternak foundation using ES-MITC3. *Latin American Journal of Solids and Structures*, 21:524. <https://doi.org/10.1590/1679-78257886>.
- Rajanna, T., Banerjee, S., Desai, Y.M., Prabhakara, D.L., (2018). Effect of reinforced cutouts and ply-orientations on buckling behavior of composite panels subjected to non-uniform edge loads, *International Journal of Structural Stability and Dynamics*, 18(04): 1850058. <https://doi.org/10.1142/S021945541850058X>.
- Rajanna, T., Banerjee, S., Desai, Y.M., Prabhakara, D., (2016b). Effects of partial edge loading and fibre configuration on vibration and buckling characteristics of stiffened composite plates. *Latin American Journal of Solids Structures*, 13(5):854-879. <https://doi.org/10.1590/1679-78252239>.
- Rajanna, T., Banerjee, S., Desai, Y.M., Prabhakara, D.L., (2016a). Vibration and buckling analyses of laminated panels with and without cutouts under compressive and tensile edge loads. *Journal of Steel Composite Structures*, 21(1):37-55. <https://doi.org/10.12989/scs.2016.21.1.037>.
- Ravi Kumar, L., Datta, P.K., Prabhakara, D.L., (2005). Vibration and stability behavior of aminated composite curved panels with cutout under partial in-plane loads. *International Journal of Structural Stability and Dynamics*, 05(01):75-94. <https://doi.org/10.1142/S0219455405001507>.
- Reddy, J.N., Phan, N.D., (1985). Stability and vibration of isotropic, orthotropic and laminated plates according to a higher-order shear deformation theory. *Journal of Sound and Vibration*, 98(2):157-170. [https://doi.org/10.1016/0022-460X\(85\)90383-9](https://doi.org/10.1016/0022-460X(85)90383-9).
- Reddy, J.N., (1996). *Mechanics of laminated composite plates*, CRC press, New York.

- Sadamoto, S., Tanaka, S., Taniguchi, K., Ozdemir, M., Bui, T.Q., Murakami, C., Yanagihara, D., (2017). Buckling analysis of stiffened plate structures by an improved meshfree flat shell formulation, *Thin walled structures*, 117: 303-313. <https://doi.org/10.1016/j.tws.2017.04.012>.
- Satish Kumar, Y.V., Mukhopadhyay, M., (1999). A new finite element for buckling analysis of laminated stiffened plates. *Composite Structures*, 46(4): 321-331. [https://doi.org/10.1016/S0263-8223\(99\)00059-8](https://doi.org/10.1016/S0263-8223(99)00059-8).
- Subash Chandra, K.S., Rajanna, T., Rao, K.V., (2020). A Parametric study on the effect of elliptical cutouts for buckling behavior of composite plates under non-uniform edge loads. *Latin American Journal of Solids Structures*, 17(08). <https://doi.org/10.1590/1679-78256225>.
- Swaminathan, K., Hirannaiah, S., Rajanna, T., (2023). Vibration and stability characteristics of functionally graded sandwich plates with/without porosity subjected to localized edge loadings. *Mechanics Based design of Structures and Machines*, 51(11):6254-6292. <https://doi.org/10.1080/15397734.2022.2038619>.
- Timoshenko, S.P., Gere, J.M., (1961). *Theory of elastic stability*, McGraw-Hill, New York.
- Shanmugam, N.E., Thevendran, V., Tan, Y.H., (1999). Design formula for axially compressed perforated plates. *Thin-Walled Structures*, 34(1):1-20. [https://doi.org/10.1016/S0263-8231\(98\)00052-4](https://doi.org/10.1016/S0263-8231(98)00052-4).
- Yathish Muddappa, P.P., Rajanna, T., Giridhara, G., (2023a). Effect of tensile and compressive nonlinear edge loads on the buckling performance of hybrid metal composite laminates with cutouts. *Mechanics Based Design of Structures and Machines*, 51(8):4294-4312. <https://doi.org/10.1080/15397734.2021.1956331>.
- Yathish Muddappa, P.P., Rajanna, T., Giridhara, G., (2023b). Effect of reinforced cutouts on the buckling and vibration performance of hybrid fiber metal laminates. *Mechanics Based Design of Structures and Machines*, 51(7):3986-4006. <https://doi.org/10.1080/15397734.2021.1948862>.
- Zhao, W., Kapania, R.K., (2016). Buckling analysis of unitized curvilinearly stiffened composite panels. *Composite Structures*, 135:365-382. <https://doi.org/10.1016/j.compstruct.2015.09.041>.
- Zhong, H., Gu, C., (2007). Buckling of symmetrical cross-ply composite rectangular plates under a linearly varying in-plane load. *Composite Structures*, 80(1):42-48. <https://doi.org/10.1016/j.compstruct.2006.02.030>.
- Zeybek, Ö., Özkılıç, Y.O., (2023). Effects of reinforcing steel tanks with intermediate ring stiffeners on wind buckling during construction. *Journal of Constructional Steel Research*, 203: 107832.